Diffraction grating-based sensing optofluidic device for measuring the refractive index of liquids

Sergio Calixto,[1*] Neil C. Bruce,[2] and Martha Rosete-Aguilar[2]

[1]*Centro de Investigaciones en Optica, Loma del Bosque 115, Leon, Gto. c.p. 37150, Mexico*
[2]*CCADET, UNAM, Apartado Postal 70 – 186, c.p. 04510, D.F., Mexico*
[*]*scalixto@cio.mx*

Abstract: We describe a simple and versatile optical sensing device for measuring refractive index of liquids. The sensor consists of a sinusoidal relief grating in a glass cell. Device calibration is done by pouring in the cell different liquids of known refractive indices. Each time a liquid is poured first order intensity is measured. The fabrication process and testing of the prototype device is described. An application in the measurement of temperature is also presented.

OCIS codes: (050.0050) Diffraction and gratings; (130.0130) Integrated optics; (120.5710) Refraction; (230.1950) Diffraction gratings.

References and links

1. F. A. Jenkins and H. E. White, *Fundamentals of Optics*, (McGraw Hill, 1957).
2. R. S. Longhurst, *Geometrical and Physical Optics* (Longman, 1973).
3. S. Nemoto, "Measurement of the refractive index of liquid using laser beam displacement," Appl. Opt. **31**(31), 6690–6694 (1992).
4. A. L. Bajor, "Refraction in plane-parallel plate - Reconsideration of method of measurement of refractive indices," Optik (Stuttg.) **124**(22), 5332–5339 (2013).
5. M. V. R. K. Murty and R. P. Shukla, "Simple method for measuring rhe refractive index of a liquid," Opt. Eng. **18**(2), 182177 (1979).
6. B. M. Pixton and J. E. Greivenkamp, "Automated measurement of the refractive index of fluids," Appl. Opt. **47**(10), 1504–1509 (2008).
7. P. Liebetraut, P. Waibel, P. H. Nguyen, P. Reith, B. Aatz, and H. Zappe, "Optical properties of liquids for fluidic optics," Appl. Opt. **52**(14), 3203–3215 (2013).
8. D. Psaltis, S. R. Quake, and C. Yang, "Developing optofluidic technology through the fusion of microfluidics and optics," Nature **442**(7101), 381–386 (2006).
9. C. Monat, P. Domachuk, and B. J. Eggleton, "Integrated optofluidics: A new river of light," Nat. Photonics **1**(2), 106–114 (2007).
10. F. Yeshaiahu, L. P. Lee, D. Psaltis, and C. Yang, *Optofluidics Fundamentals, Devices, and Applications* (McGraw Hill, 2010).
11. K. S. Chao, T. Y. Lin, and R. J. Yang, "Two optofluidic devices for the refractive index measurement of small volume of fluids," Microfluid. Nanofluidics **12**(5), 697–704 (2012).
12. C. Grillet, P. Domachuk, V. Ta'eed, E. Mägi, J. Bolger, B. Eggleton, L. Rodd, and J. Cooper-White, "Compact tunable microfluidic interferometer," Opt. Express **12**(22), 5440–5447 (2004).
13. A. Llobera, R. Wilke, and S. Büttgenbach, "Poly(dimethylsiloxane) hollow Abbe prism with microlenses for detection based on absorption and refractive index shift," Lab Chip **4**(1), 24–27 (2004).
14. S. Calixto, M. Rosete-Aguilar, D. Monzon-Hernandez, and V. P. Minkovich, "Capillary refractometer integrated in a microfluidic configuration," Appl. Opt. **47**(6), 843–848 (2008).
15. S. Calixto, M. Rosete-Aguilar, F. J. S. Marin, M. C. Solano, and C. L. Mariscal, "Refractive index mesurements through image analysis with an optofluidic device," Opt. Express **20**(3), 2073–2080 (2012).
16. P. Polynkin, A. Polynkin, N. Peyghambarian, and M. Mansuripur, "Evanescent field-based optical fiber sensing device for measuring the refractive index of liquids in microfluidic channels," Opt. Lett. **30**(11), 1273–1275 (2005).
17. S. Dante, D. Duval, B. Sepúlveda, A. B. González-Guerrero, J. R. Sendra, and L. M. Lechuga, "All-optical phase modulation for integrated interferometric biosensors," Opt. Express **20**(7), 7195–7205 (2012).
18. K. Chaitavon, S. Sumriddetchkajorn, and J. Nukeaw, "Built-in-mask microfluidic chip for highly sensitive young interferometry-based refractometer structure," Procd IEEE Sensors Conf. **6**, 2164-2167 (2012).
19. K. Misiakos, I. Raptis, E. Makarona, A. Botsialas, A. Salapatas, P. Oikonomou, A. Psarouli, P. S. Petrou, S. E. Kakabakos, K. Tukkiniemi, M. Sopanen, and G. Jobst, "All-silicon monolithic Mach-Zehnder interferometer as a refractive index and bio-chemical sensor," Opt. Express **22**(22), 26803–26813 (2014).

#253315 Received 4 Nov 2015; revised 18 Dec 2015; accepted 22 Dec 2015; published 5 Jan 2016

20. S. Calixto and C. Menchaca, "Infrared recording of transient and permanent interference gratings with commercial plastics," Appl. Opt. **28**(20), 4370–4374 (1989).
21. J. W. Goodman, *Introduction to Fourier Optics,* 2nd ed. (McGraw-Hill, 1996) pp. 73–75.
22. J. W. Goodman, *Introduction to Fourier Optics,* 2nd ed. (McGraw-Hill, 1996) pp. 81–83.
23. R. Bracewell, *The Fourier Transform and its Applications* (McGraw-Hill, 1965) pp. 104–107.
24. S. K. Mitra, N. Dass, and N. C. Varsh, "Temperature dependence of the refractive index of water," J. Chem. Phys. **57**(4), 1798–1799 (1972).
25. P. Schiebener, T. Straub, J. M. H. Leveltstengers, and J. S. Gallagher, "Refractive index of water and steam as a function of wavelength, temperature and density," J. Phys. Chem. Ref. Data **19**(3), 677–715 (1990).

1. Introduction

An important physical characteristic of liquids is their refractive index. It is one of the properties that can be used to infer the nature of liquids. Refractometry deals with the determination of the optical refractive index (n) of substances or mixture of substances. The instrument used to measure the refractive index is a refractometer. Refractometers are based on different methods which fall into two broad categories a) goniometric and interferometric. In the former method measurements are made by determining the change in direction of a beam of light, while in the interferometric method measurements are made by determining directly the retardation resulting from the transmission of light through the medium. Refractometers based on the critical angle phenomenon are, for example, the Pulfrich, Abbe, Wollaston cube prism and Geake circular prism [1, 2]. Refractometers based on interferometry are the Jamin, Mach Zehnder and Rayleigh [1]. This last refractometer is often used to measure small differences in refractive index of liquids and gases. Other class of refractometers are based on the lateral displacement of a light beam [3, 4] and angular deflection [5]. Recently two automated measurements of the refractive index of fluids based on Hilger – Chance refractometer and Critical angle method have been mentioned [6, 7].

In the last few years, new optical elements, based on liquids, have been suggested and demonstrated. These elements belong to the field of optofluidics [8–10]. Some of these elements have been applied to refractometers [11–15].

Reference 16 mentions a sensor based on a single mode optical fiber, tapered to submicrometer dimensions, and immersed in a transparent polymer. A channel for the liquid analyte is created in the immediate vicinity of the taper waist. Light propagating through the tapered section extends into the channel, making the optical loss in the system sensitive to the refractive – index difference between the polymer and the liquid. They estimated an accuracy of refractive – index measurement of 5×10^{-4}. Other microfluidic sensor is based on waveguides [17]. An integrated Mach Zehnder interferometer is built where in one arm the liquid flows. Laser diodes are used as light sources . Laser optical cavity temperature is kept constant with a temperature controller. Precision microposition stages allow alignment of the photodiode. Different wavelengths of the output light are present when the driving currents are changed. Theoretically this device will give a sensitivity of of 1.9×10^{-7} RIU but experimentally it gave 5×10^{-4} RIU. Other microfluidc refractometer was bulit with two microchannels acting as a Young double slit [18]. One channel is empty and through the second one a liquid flows. Light from a coherent source is sent to the double slit and in the far field a cosinusoidal interference pattern falls on a CCD. This CCD sens the spatial distribution of light. Resolution of this device is about 8.1×10^{-6} RIU.

Another refractometric microfluidic device also based on a Mach Zehnder interferometer is mentioned in reference [19]. Interferometer is monolitically integrated on silicon. Light source is broad-band. They used avalanche LEDs, silicon nitride waveguides and silicon p/n junctions detectors. The sensitivity, or Limit Of Detection (LOD), of this device is 1.09×10^{-5} RIU.

In this paper we propose a new method, to our knowledge, to measure the refractive index of liquids. It is based on the use of diffraction gratings immersed in the liquid to be tested. The device fabrication method is described in section 2. Section 3 shows the physical principle of the method and theoretical basis. Section 4 outlines the device characterization

#253315 Received 4 Nov 2015; revised 18 Dec 2015; accepted 22 Dec 2015; published 5 Jan 2016

method and section 5 shows an application to the measurement of temperature. In section 6 we conclude.

2. Device fabrication method

Device configuration is shown schematically in Fig. 1. A He- Ne laser is used as a light source. A sinusoidal relief grating is in a glass cell where at characterization time some liquids with known refractive index are injected. The cell had dimensions of about 12 mm X 10 mm X 10 mm. The diffraction grating had dimensions of about 8 mm X 8 mm X 5 mm. Cell and diffraction grating could be smaller. Grating could just cover the width of the illuminating beam.

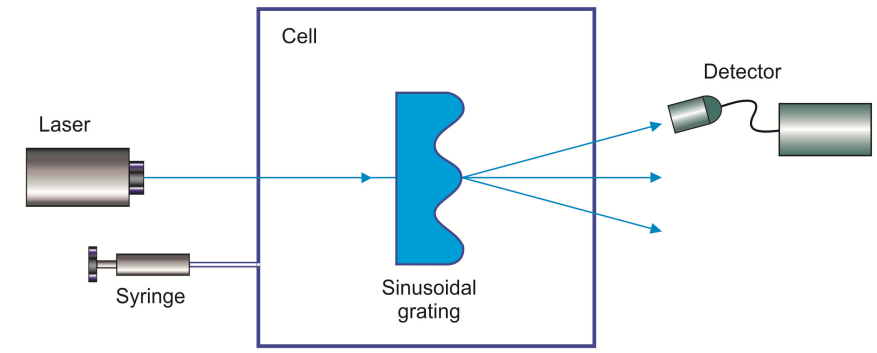

Fig. 1. Refractometer diagram showing the basic elements. Liquids are injected through a syringe. Detector measures the first order intensity.

The relief diffraction grating was fabricated with the help of a CO_2 laser. A two beam interference set up was used, Fig. 6 [20].

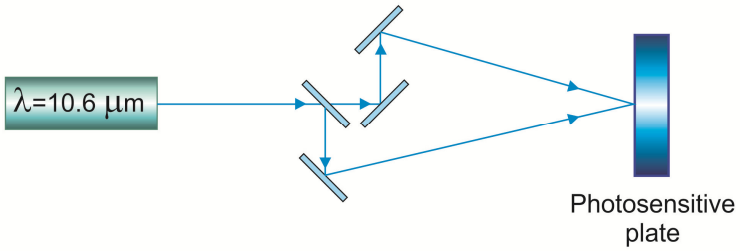

Fig. 2. Configuration useed to record the sinusoidal infrared pattern.

Material used to record the infra red sinusoidal interference pattern was Lexan (polycarbonate, refractive index 1.592) (Fig. 2). A set of gratings with different spatial frequencies and modulations were fabricated. The ones used in the experiments had a distance between crests of 260 μm (about 3.8 l/mm), with a depth modulation of 1.25 μm, and other grating with a distance between crests of 117 μm (about 8.5 l/mm) and a modulation of 0.425 μm. Figure 3(a) shows the profile of a grating surface given by an Atomic Force Microscope (AFM). It is not possible to see the full distance between crests because the longest distance measured with the microscope is about 100 μm. In Fig. 3(b) is shown one of the fabricated diffraction gratings. In Fig. 3(c) are seen the diffracted orders given by the grating when it was illuminated with light from a He – Ne. It is possible to see orders + 2, + 1, 0, –1, –2. This implies that the profile of the grating is close to a sinusoidal shape.

#253315 Received 4 Nov 2015; revised 18 Dec 2015; accepted 22 Dec 2015; published 5 Jan 2016

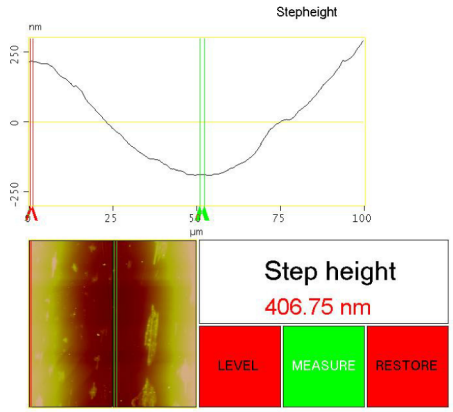

a)

b)

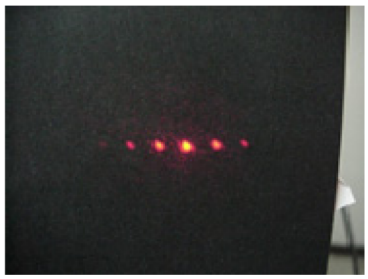

c)

Fig. 3. a) Profile and plain view of a grating with a pitch of 117 µm given by an AFM. b) Photograph of a fabricated grating. c) Diffracted orders given by the grating.

#253315 Received 4 Nov 2015; revised 18 Dec 2015; accepted 22 Dec 2015; published 5 Jan 2016

3. Physical principle of the method and theoretical basis

The basis of the proposed device is a sinusoidal relief grating immersed in liquids with different refractive indices. Schematically the phenomenon is depicted in Fig. 4.

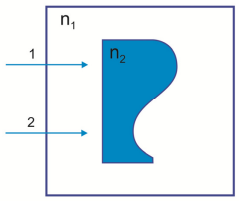

Fig. 4. Diagram shows a cycle of the diffraction grating. Two trajectories are shown. Refractive index n_2 is larger than refractive index n_1.

Phase of light passing through trajectory 1, i.e. through a crest, will suffer a longer retardation than light passing through trajectory 2. The modulation of the phase is determined by the profile of the index of refraction of the grating. If the index of refraction of the fluid filling the grating channels matches that of lexan (polycarbonate), the material with which the grating is made, then the phase will not be modulated and the device will transmit light without diffracting it.

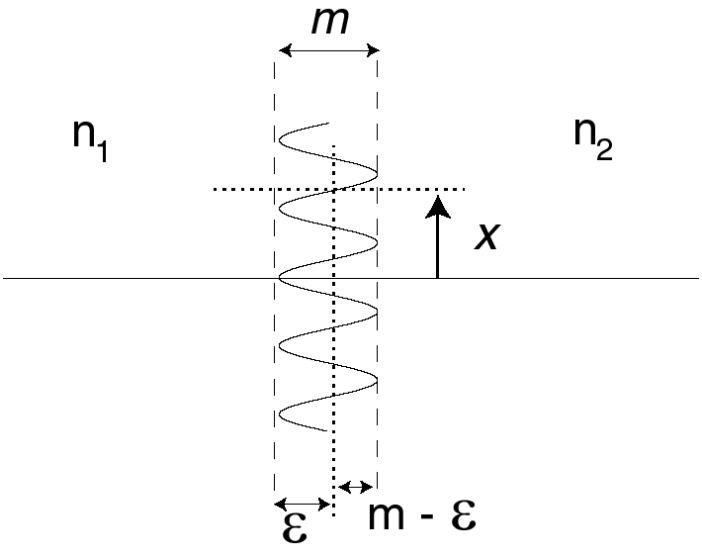

Fig. 5. Sinusoidal relief diffraction grating parameters.

Using the thin phase screen approximation, the grating only changes the phase of the rays passing through; there is no change in amplitude. Then, from the Fig. 5, the phase change between the two vertical planes shown by dashed lines is:

$$\varphi = \frac{2\pi}{\lambda_0}\left(n_1\varepsilon + n_2\left(m-\varepsilon\right)\right) \tag{1}$$

where λ_0 is the wavelength of the incident light in air, n_1 and n_2 are the refractive indices of the two media and m and ε are defined in the figure. The grating surface is a sinusoidal shape so that:

#253315 Received 4 Nov 2015; revised 18 Dec 2015; accepted 22 Dec 2015; published 5 Jan 2016

$$\varepsilon = \frac{m}{2}\sin\left(2\pi f x\right) \tag{2}$$

where f is the spatial frequency (lines/mm) of the grating shape. Then,

$$\varphi = \frac{2\pi}{\lambda_0}\left(n_2 m + \frac{m}{2}\left(n_1 - n_2\right)\sin\left(2\pi f x\right)\right) \tag{3}$$

Assuming a plane wave, of amplitude 1, normally incident, the field in the plane of the grating is given by:

$$U_i\left(x\right) = \exp\left(i\frac{2\pi}{\lambda_0}n_2 m\right)\exp\left(i\frac{2\pi}{\lambda_0}\frac{m}{2}\left(n_1 - n_2\right)\sin\left(2\pi f x\right)\right) \tag{4}$$

The far-field diffraction pattern is proportional to the scaled Fourier Transform of the field in the plane of the grating [21]

$$U\left(P\right) \propto \Im\left\{\exp\left(i\frac{2\pi}{\lambda_0}n_2 m\right)\exp\left(i\frac{2\pi}{\lambda_0}\frac{m}{2}\left(n_1 - n_2\right)\sin\left(2\pi f x\right)\right)\right\} \tag{5}$$

where $\Im\{\ \}$ indicates Fourier Transform and the spatial frequency in the diffraction plane is given by $u = {x'}/{\lambda_0 z}$, with x' the x-position on the detection plane, and z the distance between the aperture and the detection plane. The first term inside the Fourier Transform is constant with respect to the variable of the transform (x) and so can be taken outside of the Fourier Transform:

$$U\left(P\right) \propto \exp\left(i\frac{2\pi}{\lambda_0}n_2 m\right)\Im\left\{\exp\left(i\frac{2\pi}{\lambda_0}\frac{m}{2}\left(n_1 - n_2\right)\sin\left(2\pi f x\right)\right)\right\} \tag{6}$$

To calculate the Fourier transform, the following substitution can be used [22]:

$$\exp\left(iC\sin\left(2\pi f x\right)\right) = \sum_{q=-\infty}^{\infty} J_q\left(C\right)\exp\left(i\,2\pi q f x\right) \tag{7}$$

where C is a constant and $J_q(\ )$ is the Bessel function of order q.

Now,

$$U\left(P\right) \propto \exp\left(i\frac{2\pi}{\lambda_0}n_2 m\right)\Im\left\{\sum_{q=-\infty}^{\infty} J_q\left(\frac{2\pi}{\lambda_0}\frac{m}{2}\left(n_1 - n_2\right)\right)\exp\left(i\,2\pi q f x\right)\right\} \tag{8}$$

Here, because of the linearity of the Fourier transform we can take the sum of the individual Fourier transform terms, and again, the first term inside the Fourier transform is independent of the variable of the Fourier transform and can be taken outside:

$$U\left(P\right) \propto \exp\left(i\frac{2\pi}{\lambda_0}n_2 m\right)\sum_{q=-\infty}^{\infty} J_q\left(\frac{2\pi}{\lambda_0}\frac{m}{2}\left(n_1 - n_2\right)\right)\Im\left\{\exp\left(i\,2\pi q f x\right)\right\} \tag{9}$$

Using the shift theorem of Fourier transforms [23], this equation can be written as

$$U\left(P\right) \propto \exp\left(i\frac{2\pi}{\lambda_0}n_2 m\right)\sum_{q=-\infty}^{\infty} J_q\left(\frac{2\pi}{\lambda_0}\frac{m}{2}\left(n_1 - n_2\right)\right)\delta\left(\frac{x'}{\lambda_0 z} - fq\right) \tag{10}$$

where $\delta(\ )$ is the Dirac delta function.

#253315 Received 4 Nov 2015; revised 18 Dec 2015; accepted 22 Dec 2015; published 5 Jan 2016

Here, the parameter q indicates the order of diffraction, so taking only $q=1$ gives the field in the first order of diffraction:

$$U(P) \propto \exp\left(i\frac{2\pi}{\lambda_0}n_2 m\right) J_1\left(\frac{2\pi}{\lambda_0}\frac{m}{2}(n_1-n_2)\right)\delta(u-f) \tag{11}$$

and the intensity diffracted in the first order is:

$$I_1(P) \propto \left[J_1\left(\frac{2\pi}{\lambda_0}\frac{m}{2}(n_1-n_2)\right)\right]^2 \tag{12}$$

It is important to note that this intensity is independent of f, the spacing of the lines on the grating, for the phase-screen approximation.

Thus formula (12) can be used to predict the behavior of the first order intensity as a function of the following parameters: m, diffraction grating modulation, λ_0, wavelength of the incident light in air, n_1, refractive index of the medium surrounding the grating and n_2 (= 1.549) the refractive index of the diffraction grating. The first case that we have chosen is to find the behavior of the first order intensity as a function of the change in refractive index of the surrounding medium n_1. Parameter is the wavelength of the illuminating light. Wavelengths considered are: λ_0 = 632.8 nm, λ_0 = 543 nm and λ_0 = 441 nm. Modulation m = 451 nm and material grating refractive index n_2 = 1.592. The result can be seen in Fig. 6.

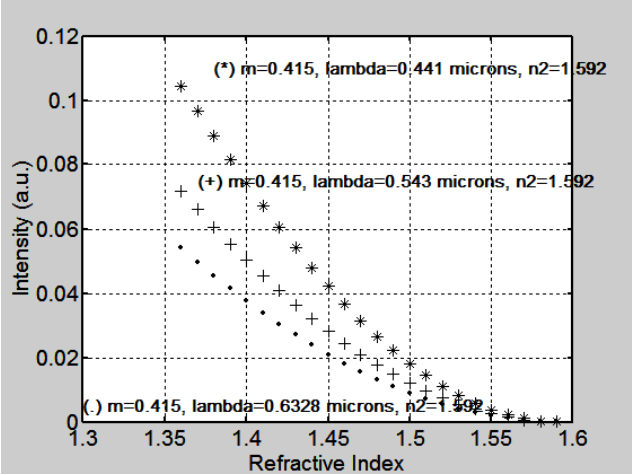

Fig. 6. Calculated first Order Intensity as a function of Refractive Index. Parameter is the light wavelength.

We can see that plots show a linear portion when values of refractive index are in the range from about 1.36 to 1.42. Thus by taking two points in each plot which lay in the linear portion we can calculate the slope of each line. Then by following the line we can find its interception with the Intensity axis. Applying this method we found the three equations that describe the linear portion of each plot. These equations are: $I_{632\ nm}$ = (–0.36 x n1) + 0.55, $I_{543\ nm}$ = (–0.43 x n1) + 0.65 and $I_{441\ nm}$ = (–0.60 x n1) + 0.92. These lines have been plotted and are shown in Fig. 7. The slope of each line represents the change of intensity as a function of the change in refractive index or the sensitivity. We can notice that the steepest slope (or the better sensitivity) is shown by the line with a slope value of –0.60. This plot corresponds when the light with the shortest wavelength is used.

#253315 Received 4 Nov 2015; revised 18 Dec 2015; accepted 22 Dec 2015; published 5 Jan 2016

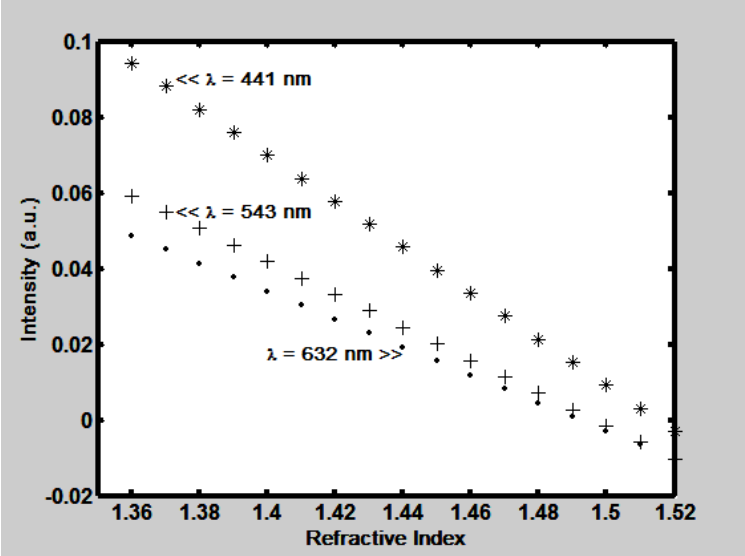

Fig. 7. Lines that represent the linear portion of the curves in Fig. 6. See text to find how they were calculated. Parameter is the light wavelength used to illuminate the grating.

The second case related with the behavior of the first order is when the grating modulation is taken as the parameter. Again using formula (12) we can predict intensity behavior considering the following values: light wavelength λ_0 = 632 nm, n2 = 1.592, n1 is the independent variable and m takes the following values: 450 nm, 1.25 mm and 1.8 mm. Results can be seen in Fig. 8.

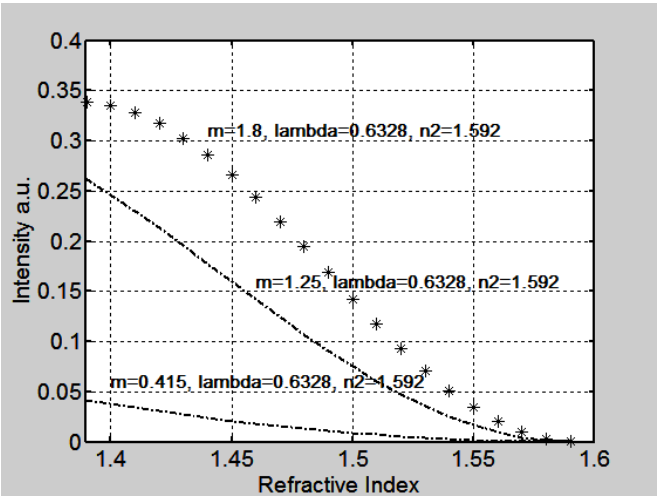

Fig. 8. Calculated First Order Intensity as a function of Refractive Index. Light wavelength is 632.8 nm. Parameter is the grating modulation m (in microns).

Again taking two points in the linear section of each plot, of each curve, we can find the slopes. The equations describing the lines are the next: $I_{m = 415nm} = (-0.33 \times n1) + 0.506$, $I_{m = 1.25\mu m} = (-1.73 \times n1) + 2.66$ and $I_{m = 1.8\mu m} = (-2.43 \times n1) + 3.78$. These lines have been plotted and are shown in Fig. 9. Thus the steepest curve is the one that was obtained with the larger modulation and has a slope of –2.43. Thus better sensitivities are obtained with larger grating modulations.

#253315 Received 4 Nov 2015; revised 18 Dec 2015; accepted 22 Dec 2015; published 5 Jan 2016

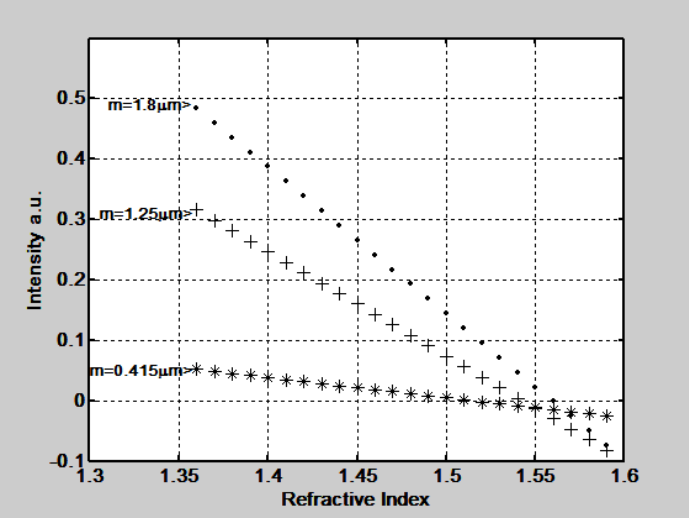

Fig. 9. Lines that represent the linear portion of the curves in Fig. 8. Line equations were obtained by considering two points in the linear portion of the curves of Fig. 8. Parameter is the grating modulation.

4. Device characterization

The calibration of the refractometric device was done with the following method. Solutions of glycerin and water with different concentrations were prepared and their refractive index was measured with an Abbe refractometer. Values of refractive indices were 1.33 (water), 1.34, 1.35, 1.36 1.37, 1.38, 1.39, 1.40, 1.41, 1.42, 1.43, 1.44, 1.45 and 1.46. Then the liquids were injected, one at a time, in the cell. After each liquid was poured first order intensity was measured with a power meter. Thus, a relation between Intensity vs Refractive Index was found. In Fig. 10 we can see a plot where the experimental and theoretical values, calculated with formula (12), are shown. The following parameters were considered: $\lambda_0 = 632nm$, $m = 415nm$. The theoretical data was normalized to the experimental data at $n = 1.36$. As can be seen from the plot, the agreement between the theory and the experiment is good. The small differences observed at small refractive indices may be due to large refraction effects because of the larger difference between the refractive indices of the two media, meaning that the phase-screen approximation is no longer valid.

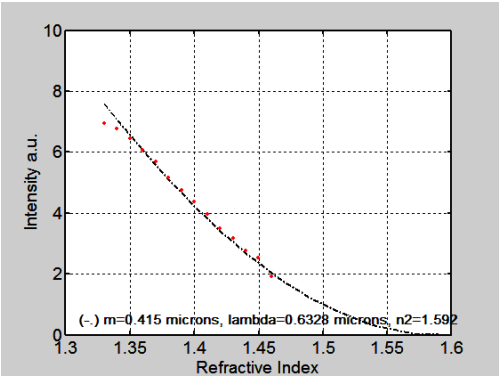

Fig. 10. Behavior of first Order Intensity as a function of Refractive Index. Experimental (red dots) and theoretical values are shown.

In section 3 we have seen that one method to improve the sensitivity of the device is by using light with short wavelengths. Thus, instead of using red light (λ = 632.8 nm) we have

#253315 Received 4 Nov 2015; revised 18 Dec 2015; accepted 22 Dec 2015; published 5 Jan 2016

chosen green light (λ = 543 nm). The behavior of Intensity as a function of Refractive Index when this wavelength was used is shown in Fig. 11 together with the plot when the red light was used. We can notice that the slope is more pronounced for green light.

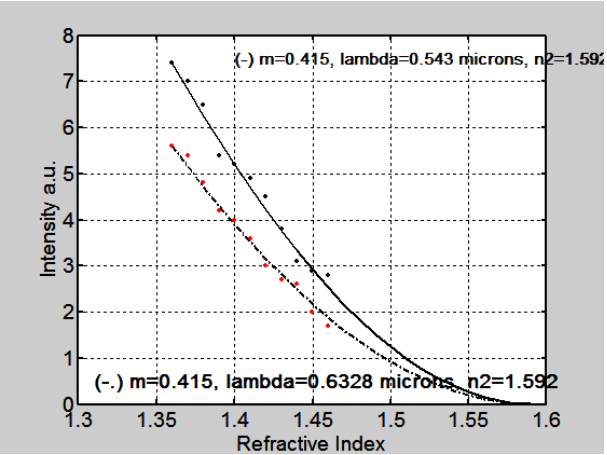

Fig. 11. Behavior of first Order Intensity vs. Refractive Index when two wavelengths are considered. Experimental and theoretical values are shown.

In section 3 we also have shown that theory predicts that with gratings showing a deeper modulation the sensitivity will be improved. We have used a grating with a modulation of m = 1.25 μm. That is a modulation 3 times the one the grating used before, Fig. 10. Results showing the behavior of first order intensity as a function of refractive index are shown in Fig. 12. Light with the wavelength (λ = 632.8 nm) has been used. By making measurements in the plots we can find that the slope for the curve when a modulation of 0.415 μm is used resulted to be – 366 μW/RIU (RIU = Refractive Index Unit). When modulation had a value of 1.25 μm the slope was −557 μW/RIU. Thus sensitivity is better when modulation is deeper.

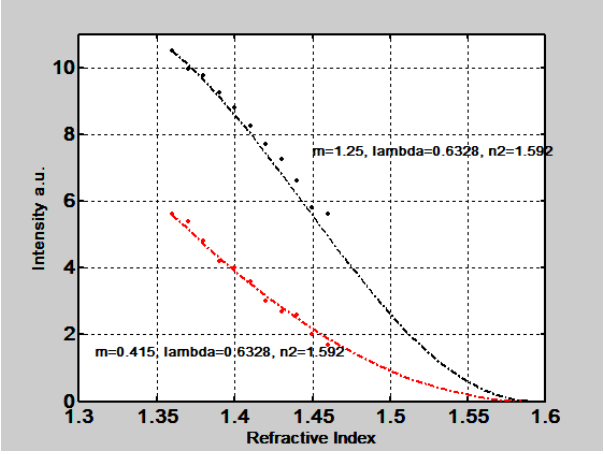

Fig. 12. Behavior of first order Intensity as a function of Refractive Index. Parameter in the plots was the grating modulation. Light with the same wavelength (λ = 632 nm) was used in both experiments.

5. Temperature measurement

Another application of the device comprising the cell and a surface relief grating was done in the calibration of the device as a function of temperature. Liquids show a decrease in density when its temperature rises. This decrease in density affects the refractive index. For example

#253315 Received 4 Nov 2015; revised 18 Dec 2015; accepted 22 Dec 2015; published 5 Jan 2016

the thermo-optic coefficient of water is about -1×10^{-4} / °C [24, 25]. To use the device as a thermometer we chose a mixture of glycerin and water, with a refractive index of 1.445, to fill the cell. Cell temperature was changed by steps from about 23 °C to about 47 °C. At the same time first order intensity was monitored. Result can be seen in Fig. 13. To have a good sensitivity a grating with a modulation depth of m = 1.25 μm and light with a wavelength of 543 nm were used.

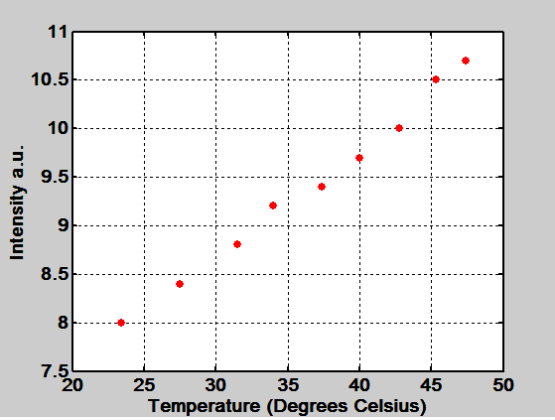

Fig. 13. Behavior of first order Intensity as a function of liquid Temperature.

5. Conclussions

We have presented a new type of refractometer based on a sinusoidal relief grating. Characterization method has shown that the best sensitivity is – 557 μW/RIU. If we suppose that the detector can measure a minimum intensity with a value of 2 μW then the Limit Of Detection (LOD) will be 3.5×10^{-3} RIU. This sensitivity can be improved when gratings with deeper modulation, light with wavelength shorter than 543 μm, or light detectors with higher sensitivity are used.

We can see that the devices mentioned at the Introduction section have a greater sensitivity than the device that we suggest in this paper. Unfortunately those devices rely on complicated and expensive fabrication methods and facilities and need electronic instruments that are expensive. Perhaps the Young interferometer is the one that is simple but when liquids with high density need to be measured the thin slits (150 μm) will be clogged. This will happen also when Mach – Zehnder interferometers with micrometer size channels are built. The sinusoidal relief grating-based device that we suggest cannot be clogged, is cheaper, has a simple structural design and fabrication process. It is versatile because it can cover various measuring ranges and various levels of sensitivities by selecting the grating modulation m or the illuminating wavelength. For some work high sensitivity and small range can be chosen and viceversa. These characteristics confer the proposed refractometer wide applicability.

Acknowledgments

We thank Edna Militza Martinez Prado and Luz Adriana Valtierra Nieto for fruitful discussions and Raymundo Mendoza for the drawings.

#253315 Received 4 Nov 2015; revised 18 Dec 2015; accepted 22 Dec 2015; published 5 Jan 2016